REPORT DOCUMENTATION PAGE

Form Approved
OMB NO. 0704-0188

1. AGENCY USE ONLY *(Leave blank)*	2. REPORT DATE	3. REPORT TYPE AND DATES COVERED
	~~6/30/98~~ 21 MAY 98	FINAL 9/1/94 - 8/31/97

4. TITLE AND SUBTITLE
Advanced Nonlinear Optical Materials Using Quasi-Phase Matching

5. FUNDING NUMBERS
DAAH04-94-G-0332

6. AUTHOR(S)
Gregory J. Salamo

7. PERFORMING ORGANIZATION NAMES(S) AND ADDRESS(ES)
Deparment of Physics
University of Arkansas
Fayetteville Arkansas 72701

8. PERFORMING ORGANIZATION REPORT NUMBER

9. SPONSORING / MONITORING AGENCY NAME(S) AND ADDRESS(ES)
U.S. Army Research Office
P.O. Box 12211
Research Triangle Park, NC 27709-2211

10. SPONSORING / MONITORING AGENCY REPORT NUMBER
ARO 33487.1-PH-DPS

11. SUPPLEMENTARY NOTES
The views, opinions and/or findings contained in this report are those of the author(s) and should not be construed as an official Department of the Army position, policy or decision, unless so designated by other documentation.

12a. DISTRIBUTION / AVAILABILITY STATEMENT
Approved for public release; distribution unlimited.

12 b. DISTRIBUTION CODE

13. ABSTRACT *(Maximum 200 words)*

We have demonstrated that screening spatial solitons in both one and two dimensions are observable using 8 nanosecond, MW optical pulses. The behavior of these high intensity pulsed screening solitons differs significantly from the previously reported low intensity c.w. screening spatial solitons, but are accurately described by their existence curve. These results will now be combined with our recent results on fixing and quasi-phase matching to generate efficient parametric conversion materials.

14. SUBJECT TERMS
Spatial soliton, photorefractive, YAG laser

15. NUMBER IF PAGES
11

16. PRICE CODE

17. SECURITY CLASSIFICATION OR REPORT	18. SECURITY CLASSIFICATION OF THIS PAGE	19. SECURITY CLASSIFICATION OF ABSTRACT	20. LIMITATION OF ABSTRACT
UNCLASSIFIED	UNCLASSIFIED	UNCLASSIFIED	UL

ADVANVED NONLINEAR OPTICAL MATERIALS

FINAL REPORT

GREGORY J. SALAMO

MAY 21, 1998

U. S. ARMY RESEARCH OFFICE

DAAH04-94-G-0332

UNIVERSITY OF ARKANSAS

APPROVED FOR PUBLIC RELEASE;
DISTRIBUTION UNLIMITED

STATEMENT OF THE PROBLEM

Recently, a new type of spatial soliton[1], based on the photorefractive effect, has been predicted and observed in both a quasi steady-state regime[2,3] and more recently in the steady state regime.[4-10] Compared to Kerr [11-14] spatial solitons, the most distinctive features of photorefractive spatial solitons are that they are observed at low light intensities (in the mW/cm^2 range) and robust trapping occurs in both transverse dimensions. Both of these attributes make photorefractive solitons attractive for applications and for fundamental studies involving the interaction between spatial solitons.[15-22] In this project we have investigated the formation of nanosecond high-intensity self-induced waveguides in order to produce materials with enhanced parametric conversion.

One transverse dimension theory of photorefractive screening solitons[5-7] predicts a universal relationship between the width of the soliton, the applied electric field, and the ratio of the soliton intensity to the sum of the equivalent dark irradiance and a uniform background intensity. We refer to this curve as the ***soliton existence curve***. This existence curve is important because experiments show that considerable deviations (~20% or more) off the curve lead to instability and breakup of the soliton beam[10,22], while much smaller deviations are typically tolerated and are "arrested" by the soliton stability properties. In the case of a low-intensity photorefractive soliton beam, i.e., intensities in the mW/cm^2 to KW/cm^2 range, recent one dimensional experiments have shown good agreement with this universal relationship.[10, 20]

Although the low-intensity feature of photorefractive spatial solitons is attractive for applications, high-intensity (MW/cm^2 to GW/cm^2) photorefractive solitons are also interesting since the speed with which the steady-state screening soliton forms is inversely proportional to the optical intensity. As we show below, solitons in SBN (strontium barium niobate) can form at nanosecond speeds for GW/cm^2 intensities. This implies that for photorefractive semiconductors, which have mobilities 100-1000 times larger than that of the photorefractive oxides, soliton formation should occur at picosecond time scales for similar intensities. For these intensities, however, the excited

free carrier density is no longer smaller than that of the acceptors and the space charge field is due both to the free carrier and the ionized donor contributions.[7]

In this project we report the first experimental observation of high-intensity screening solitons, along with a comparison between experimental results and theoretical predictions. To be in the high intensity regime, one must satisfy the requirement that $1/r << a(u_o^2+1) << 1$, where $r = N_d/N_A$, $a = s\,\frac{(I_{dark} + I_b)}{\gamma N_d}$, N_d the total donor number density, N_A, the number density of negatively charged acceptors that compensate for the ionized donors, u_o^2 is the ratio of the soliton intensity to the sum of the dark and background intensities, I_b the background intensity (used to control the effective dark carrier density), I_{dark} the dark intensity, s the photoionization cross section, and γ the recombination rate coefficient. In our case, bright high intensity solitons in photorefractive SBN can be realized at incident intensities of the order of 100 MW/cm^2 on a background of $I_b \sim$ 10MW/cm^2, which results in free-electron densities (for T~300K) of 10^{17} cm^{-3} in the center of the soliton and 10^{16} cm^{-3} far from the center. For the experiment reported here, we have used a crystal with $N_d \sim 10^{18}$cm^{-3} and $N_A \sim 10^{15}$cm^{-3} ($r=10^3$ and $a \sim 0.1$).

For the experiment a Q-switched YAG laser is used to generate a high intensity 8 ns second harmonic pulse at 530-nm which is split into two beams. One beam acts as the soliton beam, while the second beam provides the background intensity. The background beam fills the entire crystal, while the soliton beam is focused with a cylindrical lens to 11 μm (FWHM) x 2mm at the crystal entrance face. The cylindrical lens is used to observe a one-dimensional (1-D) soliton. That is, the beam is essentially infinite in extent in the vertical or **b**-direction and 11μ in the horizontal or **c**-direction. Both beams propagate along the crystalline **a** axis (for SBN **a** = **b**) and the electric field is applied along the **c** axis. The soliton beam is extraordinarily polarized in order to take advantage of the crystal large r_{33} electro-optic coefficient, while the background beam is ordinarily polarized, making it possible to select only the soliton beam for observation by using a polarizer. In particular, the soliton beam is observed using an imaging lens to image and magnify the intensity distribution at the crystal entrance and exit faces. Fig. 1 shows

typical experimental results of the entrance intensity waveform, the exit intensity waveform without trapping (zero voltage), and the exit intensity waveform with trapping (when 1500 volts are applied to the crystal between electrodes separated by 6mm). The waveforms shown evolved using 8 ns pulses at an intensity of 100MW/cm^2 after 10 pulses.

SUMMARY OF THE MOST IMPORTANT RESULTS

While it takes 10 pulses to reach the steady-state condition, the intensity of illumination during each pulse is in the high intensity regime and the beam diameter reaches e^{-1} of its steady-state value during the first pulse. Moreover, the crystal dark current is so small that the measured beam diameter at the end of each pulse, was found to be independent of the time between pulses over a range from 0.1s to 1000s. For these two reasons, our crystal can be considered to be in effective illumination at 100 MW intensities for a period of 80 ns before steady-state is reached.

One dimensional high intensity screening solitons obey the normalized nonlinear wave equation[7]

$$d^2u/d\xi^2 + \delta u - u/(1+u^2)^{1/2} = 0 \qquad (1)$$

where $u(\xi)$ is the soliton amplitude (as a function of the transverse coordinate ξ) divided by the square root of the sum of the background and dark intensities, u_0 is $u(\xi=0)$, $\delta = 2[(u_0^2+1)^{1/2}-1]/u_0^2$, and $\xi=x/d$ where we have the following: $d=(k^2 n_b^2 r_{eff} V/\ell)^{-1/2}$, $k=2n_b/\lambda$, λ is the free-space wavelength, n_b is the unperturbed refractive index, r_{eff} is the effective electro-optic coefficient for the geometry of propagation, V is the applied voltage, and ℓ is the width of the crystal between the electrodes. Equation (1) can be integrated numerically to obtain the spatial profile of the soliton and the full width at

half-maximum (FWHM) of the intensity as a function of u_0, which is the soliton existence curve. These results are shown in Fig. 2 (solid curve) for the range $0.1 \leq u_0 \leq 100$, along with the low intensity case, (dotted curve), for comparison. The difference in the two theoretical curves is because the change in the refractive index, Δn, is proportional to $(1+u^2)^{-1/2}$ for the high-intensity solitons of Fig. 2, whereas for low intensity screening solitons Δn is proportional to $(1+u^2)^{-1}$. Our experimental results with 1D solitons of the same width and wavelength and in the very same crystal for both low and high intensity solitons are marked by the open and filled squares, respectively, in Fig. 2. It is apparent that there is good agreement between experiments and theory for both the high and low intensity cases. The predominant reason for the discrepancy is that the background beam is slightly guided by the refractive index change induced by the soliton[10] (since r_{13} is not zero), rather than maintaining a constant value across the beam as is assumed theoretically.

While both the low and high intensity bright screening solitons depend on the ratio of the soliton peak intensity to the background plus the dark intensity, there are three striking differences. The first is that the lowest voltage required for trapping a bright soliton is obtained when this ratio is ≈ 2.4 in the low intensity regime and ≈ 5.5 in the high intensity regime. Indeed, in our experiments this "most favorable point" in the high intensity regime is shifted towards higher intensity ratio values as compared to the low intensity curve. Second, since the dark irradiance is extremely low in SBN, i.e., milliwatts per square centimeter (or less), the low intensity regime can, in principle, be reached without the use of a background beam (I_b=0). For the high intensity case, however, the background beam is essential and is many orders of magnitude higher than the dark intensity. Third, the slope of the low intensity curve is significantly greater than the corresponding slope for the high intensity regime when $u^2_0 > 5$. This difference in slope, for example, leads to a soliton width in the high intensity regime that is substantially lower than the corresponding soliton width in the low intensity regime for a

given intensity ratio. As seen in Fig. 2, this difference in slope is one of the striking differentiating features supported by the experimental results presented in this paper. Since precise theoretical predictions only exist for the 1-D case, a 1-D experiment was necessary for a valid comparison with theory. However, 2-D high intensity screening solitons are even more interesting, both for fundamental reasons and for applications. Fig. 3 shows typical results for a 2-D high intensity experiment for the same conditions as the 1-D experiment. Although not shown in Fig. 2, the slope of the experimental 2-D high intensity existence curve, when $u^2_0 > 5$, was identical to the 1-D high intensity case.

In conclusion, we have demonstrated that screening spatial solitons in both one and two dimensions are observable using 8 nanosecond, MW optical pulses. The behavior of these high intensity screening solitons differs significantly from the previously reported low intensity c.w. screening spatial solitons, but are accurately described by their existence curve. These results, will now be combined with quasi-phase matching to generate efficient parametric conversion materials.

PUBLICATIONS

1. One-dimensional steady-state photorefractive screening solitons, K. Kos, H. Meng, G. Salamo, M. Shih, and M. Segev, **Phy. Rev.E, 53,Rapid Comm.**,R4330, 1996.
2. The primarily-isotropic nature of photorefractive screening solitons and the interactions between them, H. Meng, G. Salamo, and M. Segev, **accepted to Optics Letters**, 1998.
3. High intensity Screening Photorefractive Solitons, K. Kos, G. Salamo, and M. Segev, **accepted to Optics Letters**, 1998.

PARTICPANTS

Mr. Konstantine Kos and Mr. Hongxing Meng were graduate students who carried out the work on this project. Mr. Meng received his Ph.D. degree at the University of Arkansas in May,1998 and Mr. Kos received his M.S. degree in January, 1998.

INVENTIONS

We have not reported or claim any inventions.

BIBLIOGRAPHY

1. R. Y. Chiao, E. Garmire, and C. H. Townes, Phys. Rev. Lett. **13**, 479 (1964).

2. M. Segev, B. Crosignani, A. Yariv, and B. Fischer, Phys. Rev. Lett. **68**, 923 (1992).

3. G. Duree, J. L. Shultz, G. Salamo, M. Segev, A. Yariv, B. Crosignani, P. DiPorto, E. Sharp, and R. R. Neurgaonkar, Phys. Rev. Lett. **71**, 533 (1993); *ibid.* **74**, 1978 (1995).

4 G. C. Valley, M. Segev, B. Crosignani, A. Yariv, M. M. Fejer, and M. Bashaw, Phys. Rev. A **50**, R4457 (1994); M. Taya, M. Bashaw, M.M. Fejer, M. Segev, and G.C. Valley, *ibid.* **52**, 3095 (1995).

5. M. Segev, G.C. Valley, B. Crosignani, P. DiPorto, and A. Yariv, Phys. Rev. Lett. **73**, 3211 (1994).

6. D. N. Christodoulides and M. I. Carvalho, J. Opt. Soc. Am. B**12**, 1628, (1995).

7. M. Segev, M. Shih, and G.C. Valley, J. Opt. Soc. Am. **13**, 706 (1996).

8. M. D. Iturbe-Castillo, P. A. Marquez-Qguilar, J. J. Sanchez-Mondragon, S. Stepanov, and V. Vysloukh, Appl. Phys. Lett. **64**, 408 (1994).

9. M. Shih, M. Segev, G.C. Valley, G. Salamo, B. Crosignani, and P. DiPorto, Elect. Lett. **31**, 826 (1995); Opt. Lett. **21**, 324 (1996).

10. K. Kos, H. Ming, G. Salamo, M. Shih, M. Segev and G. C. Valley, Rapid Comm., Phys. Rev. E **53**, R4330 (1996).

11. J. S. Aitchison, A. M. Weiner, Y. Silberberg, M. K. Oliver, J. L. Jackel, D. E. Leaird, E. M. Vogel, and P. W. E. Smith, Opt. Lett. **15**, 471 (1990).

12. G. A. Swartzlander, Jr., D. R. Anderson, J. J. Regan, H. Yin, and A. E. Kaplan, Phys. Rev. Lett. **66**, 1583 (1991).

13 R. De La Fuente, A. Barthelemy, and C. Froehly, Opt. Lett. **16**, 793 (1991).

14. B. Luther-Davies and Y. Xiaoping, opt. Lett. **17**, 496 (1992).

15. M. Shih, and M. Segev, Opt. Lett. **21**, 1538 (1996).

16. M. Shih, Z. Chen, M. Segev, T. H. Coskun, and D. N. Christodoulides, Appl. Phys. Lett. **69**, 4151 (1996).

17. M. Shih, M. Segev, and G. Salamo, Phys. Rev. Lett. **78**, 2551 (1997).

18. G. S. Garcia-Quirino, M. D. Iturbe-Castillo, V. A. Vyslouokh, J.J. Sanchez-Mondragoon, S. I. Stepanov, G. Lugo-Martinez and G. E. Torres-Cisneros, Opt. Lett. **22**, 154 (1997).

19. W. Krolikowski and S. A. Holmstrom, Opt. Lett. **22**, 369 (1997)

20. H. Meng, G. Salamo, M. Shih, and M. Segev, Opt. Lett. **22**, 448 (1997).

21. D.N. Christodoulides, S.R. Singh, M.I. Carvalho, and M. Segev, Appl. Phys. Lett. **68**, 1763 (1996).

22. Z. Chen, M. Segev, T. Coskun and D. N. Christodoulides, Opt. Lett. **21**, 1436 (1996).

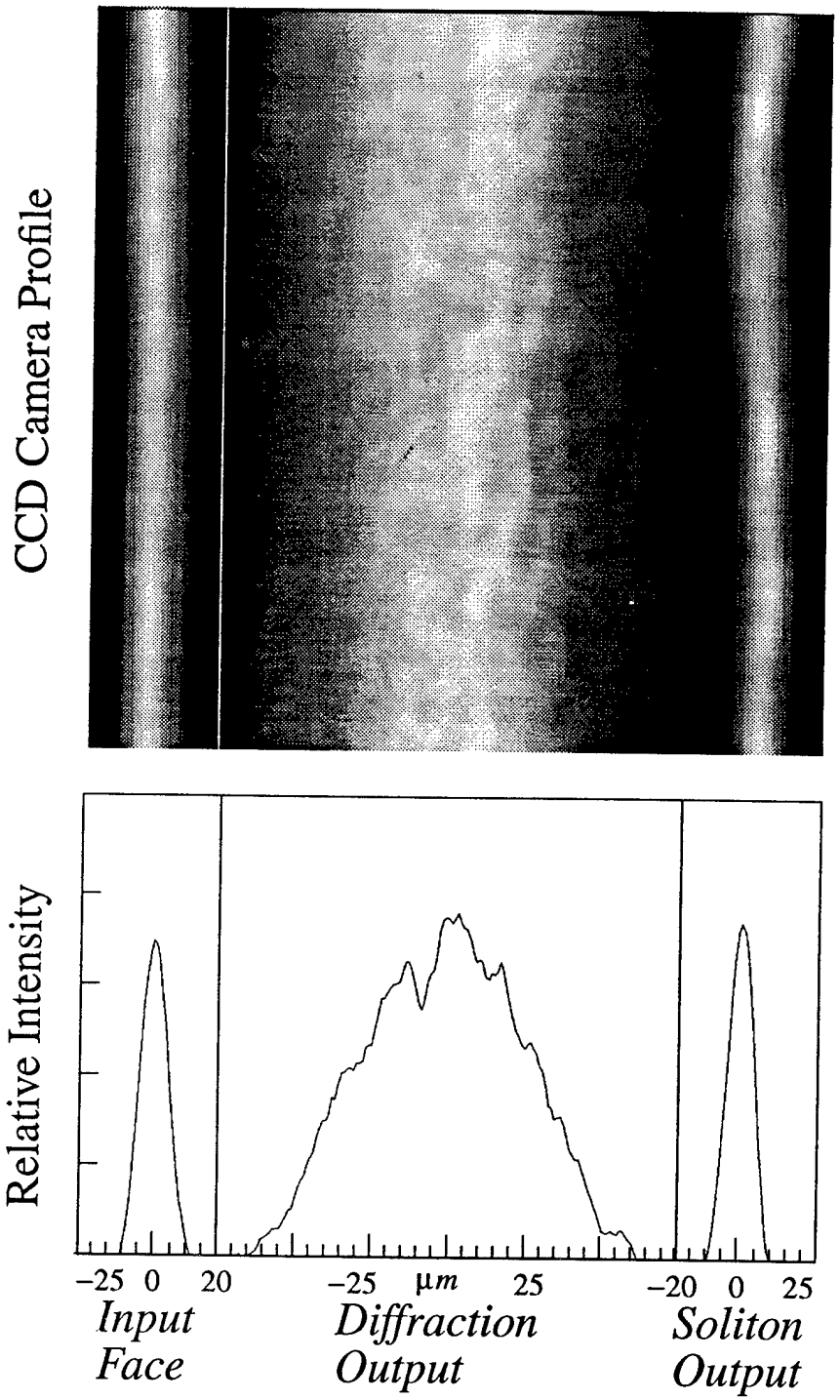
CCD Camera Profile
Relative Intensity
–25 0 20
–25 μm 25
–20 0 25
Input Face
Diffraction Output
Soliton Output

FIGURE 1

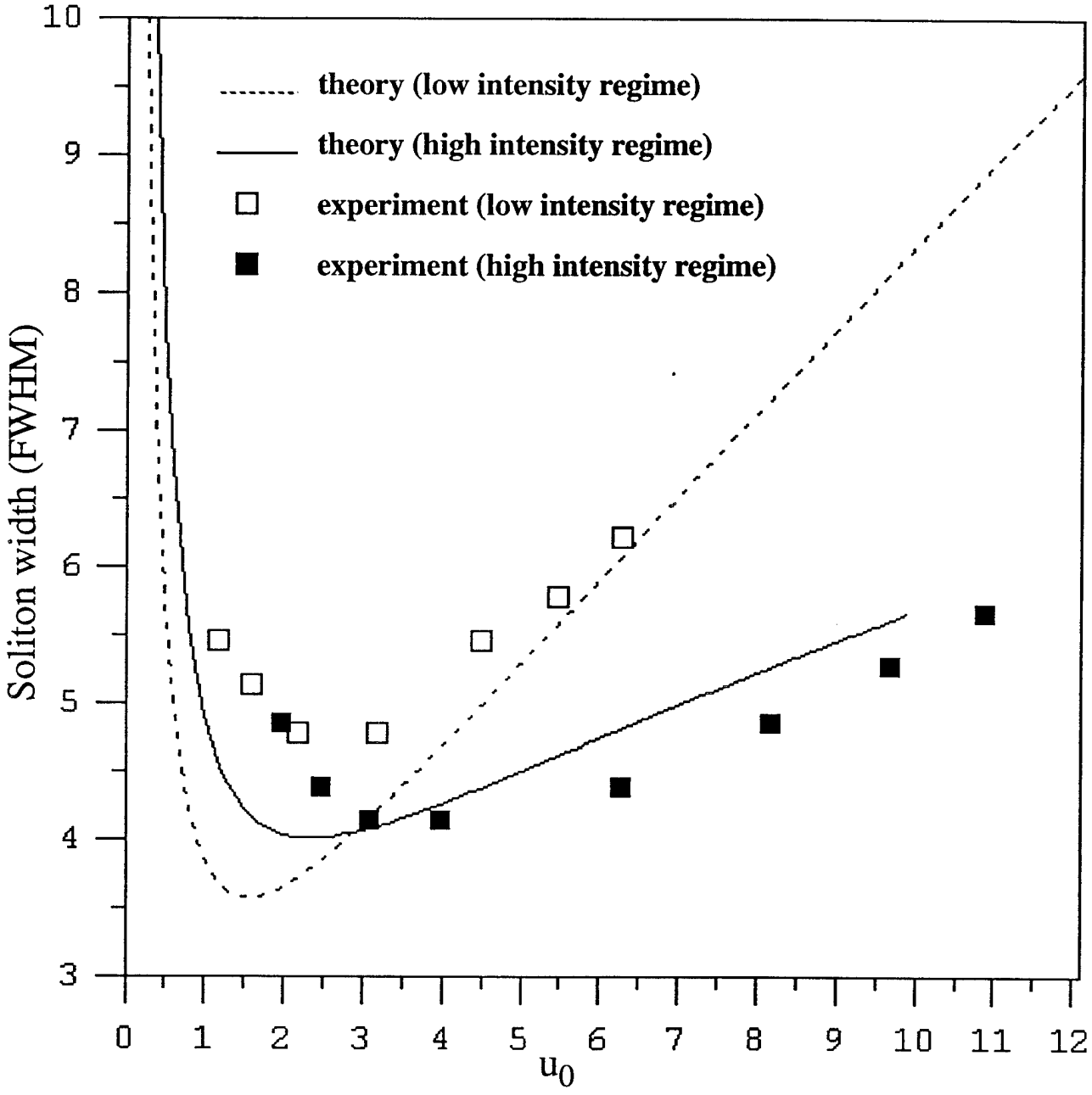
theory (low intensity regime)
theory (high intensity regime)
experiment (low intensity regime)
experiment (high intensity regime)
Soliton width (FWHM)
u_0
10
9
8
7
6
5
4
3
0
1
2
3
4
5
6
7
8
9
10
11
12

FIGURE 2

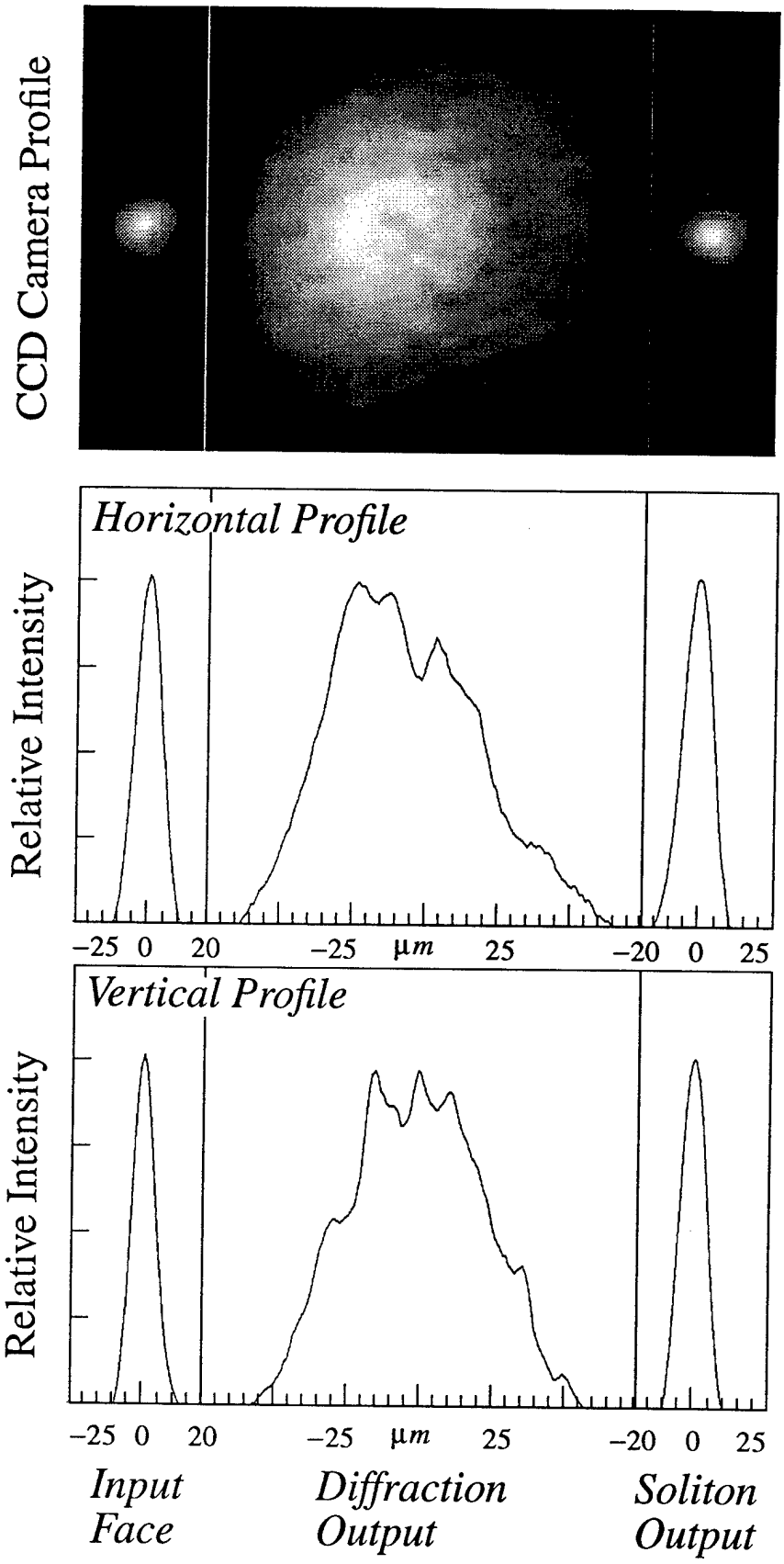
CCD Camera Profile
Horizontal Profile
Relative Intensity
−25 0 20
−25 μm 25
−20 0 25
Vertical Profile
Relative Intensity
−25 0 20
−25 μm 25
−20 0 25
Input Face
Diffraction Output
Soliton Output

FIGURE 3